Biosensors and Bioelectronics 142 (2019) 111572

Contents lists available at ScienceDirect

Biosensors and Bioelectronics

journal homepage: www.elsevier.com/locate/bios

Immobilization-free, split-mode cathodic photoelectrochemical strategy combined with cascaded amplification for versatile biosensing

Fang Li[1], Tianli Liu[1], Hong Wang, Yuming Dong, Guang-Li Wang*

International Joint Research Center for Photoresponsive Molecules and Materials, Key Laboratory of Synthetic and Biological Colloids (Ministry of Education), School of Chemical and Material Engineering, Jiangnan University, Wuxi, 214122, China

ARTICLE INFO

Keywords:
BiOI
Cathodic photoelectrochemistry
Split-mode
Cascade amplification

ABSTRACT

We propose herein an immobilization-free, split-mode cathodic photoelectrochemical (PEC) strategy coupled with a cascaded amplification for versatile biosensing. Taking DNA and microRNA (miRNA) as the model targets, the hybridization between the targets and the hairpin probe triggers the digestion of the probe DNA by T7 exonuclease (T7 Exo), thus to generate G-quadruplex (G4) forming sequences, and then the released targets (DNA or miRNA) initiate the subsequent cycling processes and generate a large amount of G4 forming sequences. Subsequently, the formed G4 sequences associate with hemin to form the G4/hemin DNAzyme, which catalytically produces 1,4-bezoquinone (BQ) for conjugating onto the surface of the chitosan (CS) deposited BiOI/ITO photocathode via the quinone-chitosan conjugation chemistry (QCCC). Under photo excitation, the covalently attached quinones can act as electron acceptors of bismuth oxyiodine (BiOI), promoting the photocurrent generation and thus allowing the elegant and "signal-on" mode for probing targets of interest. Highly sensitive and selective PEC bioassays are readily realized, with the detection limits down to 2.2 fM (for DNA) and 0.2 fM (for miRNA). Since no labeling and no electrode modification processes are needed, this split-mode PEC biosensing strategy is amenable to convenient, time/labor saving, and high-throughput detections. More significantly, it provides a novel concept to design immobilization-free and label-free cathodic PEC biosensing systems, and showcases promise in general and versatile bioanalysis research.

1. Introduction

Among various DNAzymes, the G-quadruplex (G4)/hemin (i.e., hemin intercalated G4), have found wide applications as the amplifying readout units of various biorecognition events, in which the G4 forming sequence (acting as the signal transduction element) has been integrated with the recognition sequence in one single-stranded oligonucleotides (Pelossof et al., 2010; Yang et al., 2011, 2017; Jia et al., 2012). Because of the versatility of the integrated recognition sequence, G4/hemin DNAzyme provides feasibility for the construction of various biosensing applications, including nucleic acids, metal ions, small organic targets, proteins, and enzymes. The photoelectrochemical (PEC) bioanalysis, a newly emerging analytical methodology with the merits of high sensitivity, low cost, and miniaturizability, has become a promisingly new research interests in scientific community (Zhang et al., 2015; Zhang et al., 2017; Zang et al., 2018). In the reported PEC bioassays involving G4/hemin DNAzyme as the signal transduction element (Liu et al., 2013; Wang et al., 2015; Zhuang et al., 2015; Zhang et al., 2019), to immobilize the recognition probes (usually the nucleic acids) for the targets on the electrode surfaces is the prerequisite to realize the signal readout, which involves not only complicated labeling/immobilization procedures but also tedious and time-consuming incubation and rinsing processes. And it is also difficult to prepare modified electrodes with good photostability. What's worse, the surface confined probes have restricted configurational freedom and are persecuted by the steric hindrance effect (Lubin et al., 2009; Ricci et al., 2007), which causes low biorecognition efficiency and thus leading to crippled performances in terms of sensitivity and linear range. Therefore, the immobilization-free PEC bioassays are highly desirable.

To date, only one anodic PEC bioassay (Ge et al., 2016) involving G4/hemin DNAzyme as the signal transduction element has been proposed for the immobilization-free detection. However, the exploration of cathodic PEC (Xu et al.,2019), a recently developed protocol with different sensing mechanism as well as enhanced anti-interference capability in contrast to the extensively studied anodic one, has not been shown. Herein, an immobilization-free cathodic PEC bioassay was

* Corresponding author.
E-mail address: glwang@jiangnan.edu.cn (G.-L. Wang).
[1] Fang Li & Tianli Liu, these authors contribute equally to this work.

https://doi.org/10.1016/j.bios.2019.111572
Received 25 June 2019; Received in revised form 1 August 2019; Accepted 3 August 2019
Available online 03 August 2019
0956-5663/

developed using the bismuth oxyiodide (BiOI) modified indium tin oxide (ITO) electrode as sensing unit and the G4/hemin DNAzyme as the signal transduction/amplification element. BiOI is a fascinating ternary oxide semiconductor in terms of its good chemical stability, low toxicity, narrow band gap (1.7–1.8 eV) and efficient visible-light harvesting capability in comparison with other bismuth oxyhalides (Dong et al., 2017; Zhang et al., 2018). The BiOI can easily exhibit n-type conductivity and has been widely used in anodic PEC detections (Zhou et al., 2014; Wang et al., 2017; Xu et al., 2017; Liu et al., 2018). By properly adjusting the synthetic conditions, BiOI can also behave the p-type conductivity characteristics (Hahn et al., 2012). Previously, the p-type BiOI consisted photocathodes were found to respond to dissolved oxygen (Yan et al., 2015; Zhang et al., 2018) and ferricyanide (Wang et al., 2019), restraining their applications merely applicable to the immobilization-based cathodic PEC bioassays. In this work, we found that the 1,4-bezoquinone (BQ) can greatly simulated the cathodic photocurrent of BiOI, which enabled us to construct the immobilization-free bioassays through our recently developed quinone-chitosan conjugation chemistry (QCCC) (Wang et al., 2018) strategy coupled with cascade amplification mediated with the T7 exonuclease (T7 Exo) and G4/hemin DNAzyme (see Scheme 1). Specifically, the hybridization of the target DNA or microRNA (miRNA) with the hairpin probe induced partial digestion (mediated by the T7 Exo) of the probe and released of the target and the G4/hemin DNAzyme sequence, subsequently triggered the next round of digestion for recycling of the analyte and releasing increased amount of DNAzyme sequence. The released DNAzyme sequence performed peroxidase-like catalytic activity with hemin for oxidizing hydroquinone to BQ, which was covalently attached on the surface of the chitosan (CS) deposited BiOI/ITO photocathode, for stimulating the photocurrent signal. This immobilization-free strategy allowed a split-mode detection, in which the bioreaction and the PEC detection were conducted in separated vessels, which not only circumvented the intrinsic drawbacks of immobilization-based PEC bioassays but also contributed to the enhanced throughput. Also, it is believed that the “signal on”, immobilization-free cathodic PEC strategy is preferable to the “turn-off” anodic one (Ge et al., 2016) in terms of sensitivity and selectivity due to its lower background and reduced chance of false positive signals. Importantly, considering the versatile function of the DNAzyme, it holds great promise to be as a general and extensible strategy for general cathodic PEC biosensing platforms with operation convenience without extra labeling or modification.

2. Experimental section

2.1. Materials and reagents

$Bi(NO_3)_3{\cdot}5H_2O$, ethylene glycol (EG), KI, KCl, hydroquinone (HQ), 1,4-benzoquinone (BQ), chitosan (CS), hemin(III), and H_2O_2 (30%, w/w) were all purchased from Aladdin (Shanghai, China). T7 exonuclease and 10× NEBuffer (500 mM KAc, 200 mM Tris acetate buffer, 100 mM magnesium acetate, 10 mM dithiothreitol, pH 7.9 at 25 °C) were received from New England Biolabs (Ipswich, USA). The single walled carbon nanotubes (SWCNTs) were obtained from Chengdu Organic Chemistry Co., Ltd. (Chengdu, China). All DNA and miRNA oligonucleotides were HPLC-purified and purchased from Sangon Biotechnology Co., Ltd. (Shanghai, China). Their sequences are listed as follows:

Probe for DNA: 5′-*GAT TTT CTT CCT TTT GTT C*AA AGC CCA **GGG TAG GGC GGG TTG GGC TTT**-3′

Target DNA: 5′-GAA CAA AAG GAA GAA AAT C-3′

Probe for miRNA-21: 5′-*TCA ACA TCA GTC TGA TAA GCT A*AA AGC CCA **GGG TAG GGC GGG TTG GGC TTT**-3′

Target miRNA-21: 5′-UAG CUU AUC AGA CUG AUG UUG A-3′

(Note: The italic part indicated above is the base pair complementary to the target, and the bold part is the sequences forming the G4 structure.)

The stock solutions of the hairpin probe (dissolved with the TE buffer (10 mM Tris–HCl, 1.0 mM EDTA, pH 7.4)) for the target DNA or the miRNA were heated at 88 °C for 10 min and gradually cooled to room temperature to dissociate any intermolecular interaction, and to form the stem-loop structured DNA.

2.2. Apparatus

Scanning electron microscopy (SEM) images were acquired on a Hitachi S-4800 high resolution scanning electron microscope (Hitachi, Japan). The X-ray diffractometer (XRD) pattern was recorded with an X'Pert Philips materials research diffractometer (Brook AXS, Germany). UV–vis absorption spectra were recorded by a TU-1901 UV–vis Spectrophotometer (Beijing, China). PEC measurements were performed with a homemade system including a 500 W Xe lamp equipped with an ultraviolet cutoff filter ($\lambda \geq 400$ nm) as the irradiation source and a CHI 800C electrochemical workstation (Shanghai, China) for recording the photocurrent. A three-electrode system including a modified ITO electrode with an area of 0.25 cm^2 serving as the working electrode, a Pt wire as counter electrode, and a saturated Ag/AgCl reference electrode was used for photocurrent acquirement.

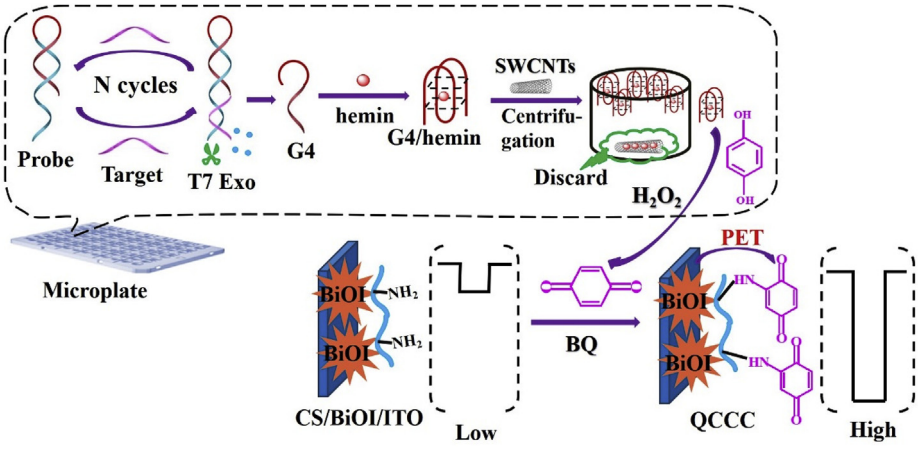

Scheme 1. Schematic illustration of the construction of the split-mode cathodic PEC sensors and the signal amplification process.

2.3. Preparation of the CS/BiOI/ITO electrode

BiOI was prepared according to the previous report with slightly modification (Hu et al., 2014). In the synthesis processes, 1.940 g of Bi $(NO_3)_3{\cdot}5H_2O$ was mixed with 40 mL of ethylene glycol (EG) solvents to obtain a white suspension. After stirring for several hours, the solutions become transparent due to that $Bi(NO_3)_3$ was dissolved in the EG solvent. Then, 0.664 g of KI dissolved in 40 mL EG solvent was added to the above solution. The mixture was further stirred for another 30 min and then put into a 150 mL Teflon-lined autoclave, which was heated and kept at 160 °C for 12 h. After cooling down to room temperature, the synthesized precipitates were washed and centrifuged by water and ethanol for several times, followed by drying at 60 °C for 12 h in oven. Finally, we used ultrapure water to disperse the collected product and acquired 1 mg/mL stock solution under ultra-sonication.

To obtain the BiOI modified ITO (BiOI/ITO) electrode, 30 μL of 1 mg/mL BiOI solution was dropped on the ITO, dried in a blast oven at 60 °C, and then cooled to room temperature. In order to attach the DNAzyme generated BQ to the surface of the BiOI/ITO electrode and achieve split detection, we used a layer of CS as a linker on the surface of the BiOI/ITO electrode to obtain the CS/BiOI/ITO electrode. To achieve this, 20 μL of CS (0.5 wt %) solution was dropped onto the BiOI/ITO electrode surface and dried at room temperature.

2.4. PEC procedures for DNA and miRNA detection

To conduct the split-mode PEC assays for DNA and miRNA, the detailed experimental procedures are as follows: In a 96-well microtiter plate, 20 μL of the hairpin probe DNA (2 μM) solution was hybridized with 20 μL of the target DNA or miRNA with varying concentrations at 37 °C for 1 h in a humidity chamber. Subsequently, 20 μL of T7 exonuclease (T7 Exo, 200 U/mL) in 1 × NEBuffer was added and incubated at 37 °C for 90 min. In the following, the resulting mixture was heated at 80 °C for 10 min to deactivate the T7 Exo. Subsequently, 100 μL of 25 μM hemin solution containing 10 mM KCl was added in the above solution and incubated for 1 h at 25 °C. Due to the guanine-rich DNA sequences of remained DNA sequences, G4/hemin-based DNAenzyme was formed. Next, 300 μL of 70 μg/mL pretreated SWCNTs was added into the G4/hemin solution and incubated for 30 min to adsorb superfluous hemin in solution. At last, the mixtures were centrifuged (12,752 rpm) for 15 min to remove redundant free hemin (Gao and Li, 2013). At this point, different amounts of G4/hemin DNAzyme that were related to the target concentration were generated for catalyzing the oxidation of HQ to generate BQ. The catalytic reaction was realized through the addition and incubation of 1.0 mM H_2O_2 and 1.0 mM HQ for 30 min at 37 °C in the microplates. Then, the CS/BiOI/ITO electrode was immersed in the above reaction mixture for 10 min and carefully washed with 0.1 mM Tris–HCl buffer solution (pH 7.0). Finally, the working electrode was immersed in the PEC cell containing 0.1 M Tris-HCl (pH 7.0) for photocurrent measurements at −0.1 V (versus saturated Ag/AgCl reference electrode).

2.5. Real sample detection

Human mastocarcinoma MCF-7 cells and Hela cells were all grown in Dulbecco's modified Eagle's medium (DMEM, purchase from GIBICO, USA) with 10% fetal calf serum (FCS) (Invitrogen, New Zealand) at 37 °C in a 5% CO_2 humid chamber. Total RNA was isolated from the cells using the Trizol reagent according to the manufacturer's instructions: After discarding the culture medium, the cells were rinsed with the sterile PBS and were added with 1 mL of Trizol, using a pipette to blow and mix the solution. Then, the lysate was allowed to stand for 5–10 min at room temperature to completely guarantee protein separation from the nucleic acids. Subsequently, 200 μL of chloroform was added to the above lysate, shaken vigorously for 15 s. After centrifuging for 10–15 min at 12,098 rpm at 4 °C, a mixture solution with different layers was obtained: the upper layer was water phase containing the RNA, and middle and lower layer were organic phase. The upper aqueous phase was transferred to the enzyme-free centrifuge tube, and an equal volume of isopropyl alcohol was added, which was placed at room temperature for 15–20 min, centrifuging for 10 min. A gel-like precipitate was formed at the bottom of the tube. After discarding the supernatant, 1 mL 75% ethanol was added to wash the obtained RNA. Ultimately, we added 30–50 μL of RNase-free distilled water to fully dissolve the RNA, and store at −70 °C for a longer time or directly used for the subsequent experiments. Using the RNA extracted from different cells as the target, similar experiments as described above were performed to test the feasibility of the designed sensor in real sample determination.

3. Results and discussion

3.1. Stimulated cathodic PEC of the BiOI microspheres through the conjugated BQ

From the X-ray diffraction (XRD) analysis and scanning electron microscope (SEM) image, we can see that the synthesized BiOI is tetragonal phase (JCPDS card no. 65-7025) (Fig. S1B) demonstrating flower-like architecture composed of assembled nanosheets with thickness of 25 nm (Fig. S1A). The obtained BiOI microspheres show distinct adsorption in the visible region and exhibit stable cathodic photocurrent under the chopped on/off illumination (Fig. S1C, Fig. S1D), demonstrating their photo to electricity conversion capability under visible light. Upon illumination, the photogenerated electrons (the minority carriers) of BiOI transfer faster towards the supporting electrolyte than that of holes (the majority carriers) with the simultaneous hole-capture by the electrons from the electrode, leading to the flow of cathodic photocurrent (Fig. 1B).

Similar to our previous report that 1,2-benzoquinone reacted with CS through the QCCC chemistry (Wang et al., 2018), we herein found that the BQ can also react nucleophilic groups of the aminopolysaccharide CS through Schiff base and/or Michael-type adduct linkage (Bittner, 2006), which led to an obvious increment in the photocurrent of the CS deposited BiOI modified ITO (CS/BiOI/ITO) electrode (Fig. 1A). The deposition of CS and the subsequent attachment of BQ on the BiOI/ITO electrode (through simply dropping CS onto the electrode surface) was certified by cyclic voltammograms (shown in Fig. S2). The peak current of the redox probe ($[Fe(CN)_6]^{3-/4-}$) decreased apparently after the deposition of CS resulted from the hindrance of CS for the diffusion of $[Fe(CN)_6]^{3-/4-}$ to the electrode surface. While the absorption spectra confirmed the attachment of BQ on CS because the absorbance of the CS film increased accompanied with the appearance of the characteristic peak for the attached BQ at 350 nm (Ghosh et al., 2012) (Fig. S3). Moreover, the distinctive oxidation (at 0.05 V versus saturated Ag/AgCl) and reduction (at −0.1 V versus saturated Ag/AgCl) peaks in accordance with that of BQ (Shimi and Park, 1997) appeared after the BQ reacted with the CS deposited BiOI/ITO electrode (Fig. 1D), further confirming the successful attachment of BQ through the linker of CS.

The amount of the deposited CS affected the PEC response of the BiOI/ITO photoelectrode to BQ, and an optimum concentration of 0.5 wt% used for electrode deposition was found (Fig. S4A). At lower concentration of CS, lower amount of BQ can be attached on the electrode surface while increased amount of CS may hinder the photo induced electron transfer between BiOI and BQ. In addition, the photoelectric communication between BQ and BiOI/ITO electrode was influenced by the applied potential and pH of the supporting electrolyte. The optimized potential applied was found at −0.1 V and the optimal pH used was 7.0 (Figs. S4B and C).

To validate that photocurrent enhancement of BiOI by BQ proceeded through the photo induced electron transfer (PET) mechanism, the conduction band (CB) potential of BiOI was revealed through linear

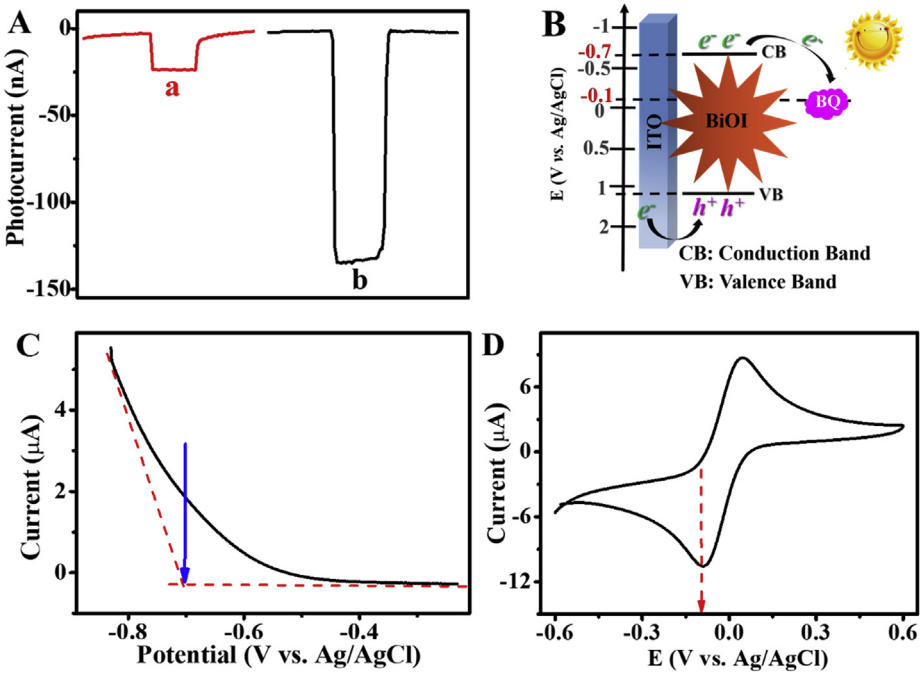

Fig. 1. (A) Photocurrent responses of the CS/ BiOI/ ITO electrode in Tris-HCl (0.1 M, pH 7.0) before (a) and after reaction with 1,4-benzoquinone (10 μM). (B) The signal generation and enhancement mechanism of the BiOI/ITO electrode by BQ. (C) Cathodic linear potential scan for determining the CB edge of the BiOI specimens in the deaerated Na_2SO_4 solution (0.2 M). (D) Cyclic voltammograms of the CS/ BiOI/ITO electrode conjugated by BQ (produced by G4/hemin catalyzed oxidization of HQ) in the deaerated Tris − HCl solution (0.1 M, pH 7.0).

potential scan (Yeh et al., 2013) and was estimated as −0.7 V versus saturated Ag/AgCl (Fig. 1C), which was similar to the previous literature (Hu et al., 2014). By comparing the CB of BiOI with the reduction potential of BQ (−0.1 V, Fig. 1D), we can see that there was a potential gradient driving the PET from the CB of BiOI to BQ. The photocurrent enhancement mechanism of BiOI by BQ is exhibited in Fig. 1A.

The photocurrent of CS/BiOI/ITO electrode responds to BQ in the linear range from 10 nM to 1.0 mM (Fig. S5) with a low detection limit of 2.0 nM. This sensitive response allowed us to construct versatile bioassays on the basis of the G4/hemin DNAzyme to catalyze the oxidation of HQ to generate BQ. Exemplified by taking DNA and miRNA as targets, the bioassays were conducted based on the cascaded amplification in homogeneous solutions: Upon the hybridization of the target (DNA or miRNA) with the corresponding hairpin probe, the T7 exonuclease (T7 Exo) digested the hydrid sequence of the probe, generating G4 forming sequences, and simultaneously released the target (DNA or miRNA) for the next cycling round. Assisted by the T7 Exo digestion for target recycling, one target can produce a large amount of G4 forming sequences; and the subsequently formed G4/hemin DNAzyme functioned as a mimicking enzyme converting to HQ to BQ (D.W. Zhang et al., 2013), forming a cascade further amplifying the signal. Considering that the superfluous hemin itself also had the catalytic ability towards HQ oxidation in the presence of H_2O_2, causing undesirable background signal, we adopted the SWNTs to selectively remove the redundant free hemin according to the literature (Gao and Li, 2013). To confirm the formation of the G4/hemin DNAzyme, UV–vis absorption spectra under different conditions were investigated. As shown in Fig. S6 (curve a), the absorption spectrum of the hemin solution contains a characteristic absorption band at 387 nm, while this typical absorption of hemin becomes stronger with the absorption peak red-shifted in the presence of the formed G4 sequence (Fig. S6, curve b), demonstrating the formation of the G4/hemin structure (L.B. Zhang et al., 2013). As shown in Fig. S7, a much higher photocurrent is observed under the coexistence of the G4 sequence and hemin (to form the G4/hemin DNAzyme) in comparison with that in the presence of G4 or hemin alone. This indicated that the high catalytic activity of the G4/hemin DNAzyme was responsible for the oxidation of HQ to BQ, while the catalytic activity of the G4 (Fig. S7, curve c) or hemin (Fig. S7, curve d) alone was too weak to catalyze the reaction between HQ and H_2O_2. Therefore, the designed protocol was conveniently and economically available for the detection of homogeneous DNAzyme catalytic reaction and can be applied for the cathodic PEC biosensor using DNAzyme as the signal reporter.

3.2. Analytical performance

Under the optimum conditions, the analytical performances of the proposed biosensors were evaluated. The calibration plot was constructed by plotting ΔI ($\Delta I = I/I_0$, where I and I_0 were the photocurrent of the detection system with and without the target, respectively) against DNA or miRNA-21 concentrations. The target DNA can be detected in a linear range from 0.01 pM to 1 nM (Fig. S8B), with the detection limit estimated to be 2.2 fM at a signal-to-noise ratio of 3. While the photocurrent responses increase linearly with the concentration of miRNA-21 ranging from 1.0 fM to 0.1 nM (Fig. 2B) with a detection limit of 0.2 fM (S/N = 3). By comparing with other reported methods for DNA and miRNA detection (Tables S1 and S2), we can see that this protocol shows competitive performances in terms of sensitivity and linear range. In addition, the selectivity of the sensor was assessed by comparing the response with different kinds of other interferents, including single-, two- or three-base mismatched DNA or miRNA sequences, which revealed good selectivity of the proposed cathodic PEC biosensor (Fig. S8C and Fig. 2C).

The feasibility of the proposed system for real sample application was examined by monitoring miRNA-21 in the lysates from two cancerous cell lines, i.e., the human breast (MCF-7) and cervical (HeLa) cancer cells. According to the results shown in Fig. 2D, the lysates from 100, 1000 or 10000 HeLa cells only cause a slight increase in the photocurrent response, indicating the low content of miRNA-21 in the HeLa cells. While the lysates from the elevated numbers (100, 1000 or 10000) of MCF-7 cells result in an obvious increase in the photocurrent response. It is convinced that the levels of miRNA-21 in the MCF-7 cells are higher than in the HeLa cells because the miRNA-21 is overexpressed in the MCF-7 cells rather than the HeLa cells (Shi et al., 2015). Therefore, the developed method may be potentially used in future for real sample detection.

4. Conclusions

In conclusion, this study demonstrates an immobilization-free, split-

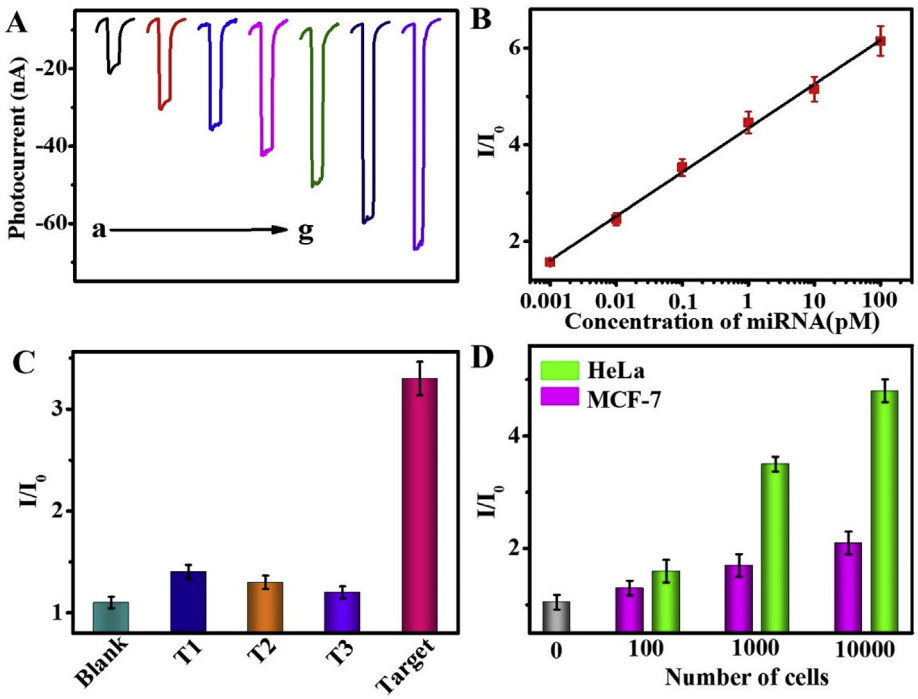

Fig. 2. (A) Photocurrent responses of the PEC sensor to different concentrations of miRNA, from a to i: 0, 0.001, 0.01, 0.1, 1, 10, 100 pM. (B) Relative calibration curve for miRNA detection. (C) Selectivity of the PEC sensing platform by comparing the response for target miRNA (1.0 pM) with base mismatched miRNA. T1, T2 and T3 is one, two or three base mismatched miRNA (10 pM), respectively). (D) Detection of miRNA-21 from lysates of different cancer cells.

type cathodic PEC biosensing platform on the basis of quinone-CS conjugation coupled with T7 Exo assisted target cycling and DNAzyme biocatalysis for cascade signal amplification. Taking the DNA and miRNA as model analytes, the CS deposited BiOI/ITO electrode served as a highly efficient photocathode that capturing and responding to the DNAzyme generated BQ, which proved to be highly sensitive and selective for PEC detection of the corresponding targets. In compassion to the widely reported immobilization-based cathodic PEC pattern, this immobilization-free strategy not only avoids complex probe labelling and electrode modification/washing procedures but also offers the benefits of enhanced accessibility, reduced time/cost, and high throughput. More significantly, the protocol proposed herein may easily extensible as a general strategy for versatile cathodic PEC bioassays that can generate DNAzyme as products.

Declaration of interest statement

The authors declare that they have no known competing financial interests or personal relationships that could have appeared to influence the work reported in this paper.

Conflict of interest

The authors declared that they have no conflicts of interest to this work.

CRediT authorship contribution statement

Fang Li: Investigation, Data curation, Writing - original draft, Formal analysis. **Tianli Liu:** Investigation, Data curation, Writing - original draft, Formal analysis. **Hong Wang:** Methodology. **Yuming Dong:** Supervision, Validation. **Guang-Li Wang:** Writing - review & editing, Supervision.

Acknowledgements

Financial supports from the National Natural Science Foundation of China (21575052, 21676123), the National First-class Discipline Program of Food Science and Technology (JUFSTR20180301), the MOE & SAFEA for the 111 Project (B13025), and the Fundamental Research Funds for the Central Universities (JUSRP21936) are appreciated.

Appendix A. Supplementary data

Supplementary data to this article can be found online at https://doi.org/10.1016/j.bios.2019.111572.

References

Bittner, S., 2006. Amino acids 30, 205–224.
Dong, R.F., Hu, Y., Wu, Y.F., Gao, W., Ren, B.Y., Wang, Q.L., Cai, Y.P., 2017. J. Am. Chem. Soc. 139, 1722–1725.
Gao, Y., Li, B.X., 2013. Anal. Chem. 85, 11494–11500.
Ge, L., Wang, W.X., Hou, T., Li, F., 2016. Biosens. Bioelectron. 77, 220–226.
Ghosh, A., Choudhury, A., Das, A., Chatterjee, N.S., Das, T., Chowdhury, R., Panda, K., Banerjee, R., Chatterjee, I.B., 2012. Toxicology 292, 78–89.
Hahn, N.T., Hoang, S., Self, J.L., Mullins, C.B., 2012. ACS Nano 6, 7712–7722.
Hu, J., Weng, S.X., Zheng, Z.Y., Pei, Z.X., Huang, M.L., Liu, P., 2014. J. Hazard Mater. 264, 293–302.
Jia, S.M., Liu, X.F., Kong, D.M., Shen, H.X., 2012. Biosens. Bioelectron. 35, 407–412.
Liu, Q., Yin, Y.Y., Hao, N., Qian, J., Li, L.B., You, T.Y., Mao, H.P., Wang, K., 2018. Sens. Actuators B Chem. 260, 1034–1042.
Lubin, A.A., Vander Stoep Hunt, B., White, R.J., Plaxco, K.W., 2009. Anal. Chem. 81, 2150–2158.
Liu, X.Q., Niazov-Elkan, A., Wang, F., Willner, I., 2013. Nano Lett. 13, 219–225.
Pelossof, G., Tel-Vered, R., Elbaz, J., Willner, I., 2010. Anal. Chem. 82, 4396–4402.
Ricci, F., Lai, R.Y., Heeger, A.J., Plaxco, K.W., Sumner, J.J., 2007. Langmuir 23, 6827–6834.
Shi, K., Dou, B.T., Yang, C.Y., Chai, Y.Q., Yuan, R., Xiang, Y., 2015. Anal. Chem. 87, 8578–8583.
Shimi, Y.B., Park, S.M., 1997. J. Electroanal. Chem. 425, 201–207.
Wang, G.L., Liu, K.L., Shu, J.X., Gu, T.T., Wu, X.M., Dong, Y.M., Li, Z.J., 2015. Biosens. Bioelectron. 69, 106–112.
Wang, G.L., Yuan, F., Gu, T.T., Dong, Y.M., Wang, Q., Zhao, W.W., 2018. Anal. Chem. 90, 1492–1497.
Wang, H., Li, F., Dong, Y.M., Li, Z.J., Wang, G.L., 2019. Sens. Actuators B Chem. 288, 683–690.
Wang, H., Ye, H.L., Zhang, B.H., Zhao, F.Q., Zeng, B.Z., 2017. J. Mater. Chem. 5, 10599–10608.
Wang, X.X., 2018. Appl. Catal. B Environ. 235, 238–245.
Xu, L., Yan, P.C., Li, H.N., Ling, S.Y., Xia, J.X., Xu, Q., Qiu, J.X., Li, H.M., 2017. RSC Adv. 7, 7929–7935.
Xu, Y.T., Yu, S.Y., Zhu, Y.C., Fan, G.C., Han, D.M., Qu, P., Zhao, W.W., 2019. Trends Anal. Chem. 114, 81–88.
Yan, K., Liu, Y., Yang, Y.H., Zhang, J.D., 2015. Anal. Chem. 87, 12215–12220.

Yang, H.T., Liu, A.R., Wei, M., Liu, Y.J., Lv, B.J., Wei, W., Zhang, Y.J., Liu, S.Q., 2017. Anal. Chem. 89, 12094–12100.
Yang, Q.L., Zhao, J., Zhou, N.D., Ye, Z.H., Li, G.X., 2011. Biosens. Bioelectron. 26, 2228–2231.
Yeh, T.F., Chen, S.J., Yeh, C.S., Teng, H., 2013. J. Phys. Chem. C 117, 6516–6524.
Zang, Y., Fan, J., Ju, Y., Xue, H., Pang, H., 2018. Chem. Eur J. 24, 14010–14027.
Zhang, D.W., Nie, J., Zhang, F.T., Xu, L., Zhou, Y.L., Zhang, X.X., 2013. Anal. Chem. 85, 11494–11500.
Zhang, L.B., Zhu, J.B., Guo, S.J., Li, T., Li, J., Wang, E.K., 2013. J. Am. Chem. Soc. 135, 2403–2406.
Zhang, L., Ruan, Y.F., Liang, Y.Y., Zhao, W.W., Yu, X.D., Xu, J.J., Chen, H.Y., 2018. ACS Appl. Mater. Interfaces 10, 3372–3379.
Zhang, L., Shi, X.M., Xu, Y.T., Fan, G.C., Yu, X.D., Liang, Y.Y., Zhao, W.W., 2019. Biosens. Bioelectron. 134, 103–108.
Zhang, N., Zhang, L., Ruan, Y.F., Zhao, W.W., Xu, J.J., Chen, H.Y., 2017. Biosens. Bioelectron. 94, 207–218.
Zhang, Y.Q., Lin, C., Lin, Q., Jin, Y.B., Wang, Y.H., Zhang, Z.Z., Lin, H.X., Long, J.L., Zhao, W.W., Xu, J.J., Chen, H.Y., 2015. Chem. Soc. Rev. 44, 729–741.
Zhou, Y.L., Xu, Z.N., Wang, M., Sun, B., Yin, H.S., Ai, S.Y., 2014. Biosens. Bioelectron. 53, 263–267.
Zhuang, J.Y., Lai, W.Q., Xu, M.D., Zhou, Q., Tang, D.P., 2015. ACS Appl. Mater. Interfaces 7, 8330–8338.